Molecular Basis for Complex Formation between Methylamine Dehydrogenase and Amicyanin Revealed by Inverse Mutagenesis of an Interprotein Salt Bridge†

Zhenyu Zhu, Limei H. Jones, M. Elizabeth Graichen, and Victor L. Davidson*

Department of Biochemistry, The University of Mississippi Medical Center, Jackson, Mississippi 39216-4505

Received March 6, 2000; Revised Manuscript Received May 10, 2000

ABSTRACT: Methylamine dehydrogenase (MADH) and amicyanin form a physiologic complex which is required for interprotein electron transfer. The crystal structure of this protein complex is known, and the importance of certain residues on amicyanin in its interaction with MADH has been demonstrated by site-directed mutagenesis. In this study, site-directed mutagenesis of MADH, kinetic data, and thermodynamic analysis are used to probe the molecular basis for stabilization of the protein complex by an interprotein salt bridge between Arg99 of amicyanin and Asp180 of the α subunit of MADH. This paper reports the first site-directed mutagenesis of MADH, as well as the construction, heterologous expression, and characterization of a six-His-tagged MADH. αAsp180 of MADH was converted to arginine to examine the effect on complex formation with native and mutant amicyanins. This mutation had no effect on the parameters for methylamine oxidation by MADH, but significantly affected its interaction with amicyanin. Of the native and mutant proteins that were studied, their observed order of affinity for each other was as follows: native MADH and native amicyanin > native MADH and R99D amicyanin > αD180R MADH and native amicyanin > αD180R MADH and R99D amicyanin, and αD180R MADH and R99L amicyanin. The αD180R mutation also eliminated the ionic strength dependence of the reaction of MADH with amicyanin that is observed with wild-type MADH. Interestingly, the inverse mutation pair of αD180R MADH and R99D amicyanin did not restore the favorable salt bridge, but instead disrupted complex formation much more severely than did either individual mutation. These results are explained using molecular modeling and thermodynamic analysis of the kinetic data to correlate the energy contributions of specific stabilizing and destabilizing interactions that are present in the wild-type and mutant complexes. A model is also proposed to describe the sequence of events that leads to stable complex formation between MADH and amicyanin.

Methylamine dehydrogenase (MADH)[1] is an enzyme in a soluble electron transfer chain of proteins that enables several Gram-negative bacteria to use methylamine as a carbon and energy source (*1*, *2*). MADH from *Paracoccus denitrificans* is a 125 kDa protein with two sets of identical subunits arranged in an $\alpha_2\beta_2$ structure.[2] Each smaller β subunit possesses a tryptophan tryptophylquinone (TTQ) prosthetic group (*2*) that participates in catalysis and electron transfer. TTQ is formed by posttranslational modification of residues Trp57 and Trp108 of the β subunit. MADH catalyzes the oxidative deamination of methylamine and electron transfer from methylamine to amicyanin, a type I blue copper protein (*3*), according to eq 1.

$$CH_3NH_3^+ + 2\text{amicyanin}_{\text{oxidized}} + H_2O \rightarrow CH_2O + 2\text{amicyanin}_{\text{reduced}} + NH_4^+ + 2H^+ \quad (1)$$

The oxidation of reduced MADH by amicyanin requires long-range electron transfer between these proteins. Since the electron acceptor for this oxidoreductase is a protein, rather than a small molecule like O_2 or NAD^+, electron transfer from reduced TTQ cannot occur directly. The reaction centers, TTQ in MADH and copper in amicyanin, are separated by 9.4 Å (*4*). The binding and electron transfer reactions of MADH with amicyanin have been the subject of many studies which have characterized: the binding constants and K_m values for complex formation under different reactions conditions (*5*−*7*), the rates and mechanisms of electron transfer from different redox forms of TTQ to copper (*8*−*11*), and complex-dependent changes in the redox properties of amicyanin (*12*). Crystal structures are also available for MADH (*13*), amicyanin (*14*), and complexes of MADH and amicyanin (*4*, *15*).

The crystal structures reveal that the interface of amicyanin and MADH is largely hydrophobic and includes amicyanin residues Met71, Met51, Met28, Pro52, Pro94, Pro96, and

† This work was supported by National Institutes of Health Grant GM-41574.

* To whom correspondence should be addressed: Department of Biochemistry, The University of Mississippi Medical Center, 2500 N. State St., Jackson, MS 39216-4505. Telephone: (601) 984-1516. Fax: (601) 984-1501. E-mail: vdavidson@biochem.umsmed.edu.

[1] Abbreviations: MADH, methylamine dehydrogenase; TTQ, tryptophan tryptophylquinone; PES, phenazine ethosulfate; DCIP, 2,6-dichlorophenolindophenol; KP_i, potassium phosphate buffer; PDB, Protein Data Bank; 6xHis-MADH, recombinant MADH with a sequence of six histidine residues inserted at the C-terminal end of the β subunit.

[2] The larger α subunit of MADH, sometimes termed the H subunit, is encoded by the *mauB* gene. The smaller β subunit of MADH, sometimes termed the L subunit, is encoded by the *mauA* gene. This paper uses the α and β terminology.

10.1021/bi000502p CCC: $19.00
Published on Web 07/06/2000

Table 1: Bacterial Strains and Plasmids

strain or plasmid	relevant features	source or reference
bacteria		
E. coli		
JM100	general cloning strain	Promega
XL-1	general cloning strain	Stratagene
S17-1	conjugation donor, *mob*$^+$, Sm^r	*26*
P. denitrificans	wild type, Sm^r	ATCC 13543
R. sphaeroides 2.4.1	wild type	laboratory strain
plasmid		
pRK415-1	broad-host-range vector, Tc^{r}IncP, pUC12/13 multiple cloning site, *lacZ*	*27*
pBSII KS/SK	general cloning strain, ColE1, Ap^r, *lac*Z	Stratagene
pMEG987	pBSII KS, *cox* II promoter, *mauFBEDACJG*	*7*
pMEG985	pUC19, *Eco*RI fragment from pMEG987	this work
pMEG977	pUC19, with *Eco*RI fragment inserted six-His tag	this work
pMEG976	pBSII KS, *cox* II promoter, *mauFBEDA6xhisCJG*	this work
pMEG975	pRK415-1, *cox* II promoter, *mauFBEDA6xhisCJG*	this work
pZZ102	PRK415-1, *cox* II promoter, *mauFBEDA6xhisCJG*, with mutation D180R in *mauB*	this work

Phe97 and MADH residues[3] αPhe143, αPro145, αAla146, αPro147, αTyr182, βAla55, βVal58, βLeu71, βAla73, βPhe102, βPhe110, and βPhe117. Site-directed mutagenesis studies of amicyanin revealed that conversion of Phe97 to glutamate decreased the affinity of MADH and amicyanin by 2 orders of magnitude (*7*), supporting the importance of these hydrophobic interactions in stabilizing complex formation. In addition to the stabilization of the complex by these hydrophobic interactions, a pair of charged residues, Arg99 of amicyanin and αAsp180 of MADH, form a salt bridge at the periphery of the hydrophobic patch. Conversion of Arg99 to either aspartate or leucine by site-directed mutagenesis also severely destabilized complex formation (*7*). These mutations not only weakened the binding but also eliminated the dependence of binding on ionic strength. The wild-type complex exhibits much stronger binding at low ionic than at high ionic strengths (*6*, *7*).

In studying MADH−amicyanin interactions, we have previously been limited to performing site-directed mutagenesis on amicyanin. The recent success in heterologous expression of recombinant MADH in *Rhodobacter sphaeroides* (*16*) provided the potential for site-directed mutagenesis of MADH as well. This paper describes the construction, expression, and properties of a new form of recombinant MADH (6xHis-MADH) which possesses a six-histidine tag at the C-terminus of the β subunit. The 6xHis-MADH is much easier to purify from cell extracts than the native recombinant MADH and allows one to also purify mutants of MADH which may be inactive or possess assembly defects.

To further examine the importance of the salt bridge between Arg99 of amicyanin and αAsp180 of MADH, and to gain insight into the possible roles of nearby surface residues in formation of this critical interprotein salt bridge, αAsp180 was converted to arginine by site-directed mutagenesis. The reaction of this mutant was studied with wild-type and mutant amicyanins, including R99D amicyanin that possesses the complementary mutation on amicyanin. The results of kinetic and thermodynamic analyses of the interactions of these proteins and molecular modeling studies are used to identify important interactions between αAsp180 and neighboring residues on MADH and amicyanin. These data are also used to develop a model for the mechanism of complex formation between MADH and amicyanin.

[3] The numbering system used here for the MADH α subunit is based on the refined crystal structure of MADH (*13*). The residue number is different from that found in Protein Data Bank files 2MTA and 2BBK. To convert to the numbering system which is used in this paper, one must add 13 to the residue number as listed in the PDB files, as well our earlier publication (*7*). For example, residue αAsp180 corresponds to αAsp167 in files 2MTA and 2BBK. The numbering for the β subunit is unchanged.

EXPERIMENTAL PROCEDURES

Materials. Native MADH and amicyanin were purified from *P. denitrificans* as described previously (*17*). Site-directed mutants of amicyanin were prepared and purified from *Escherichia coli* as described previously (*7*). Native recombinant MADH was prepared and purified from *R. sphaeroides* as described previously (*16*).

Construction of a Plasmid To Express 6xHis-MADH. Recombinant MADH is expressed from the plasmid pMEG987 (*16*), a pBluescript derivative which contains the genes *mauFBEDACJG* (Table 1). A 653-base *Eco*RI fragment which contains 95 bases from the 3′ end of *mauA*, the gene which encodes the MADH β subunit, was excised and inserted into pUC19 to form pMEG985. This plasmid is much smaller than pMEG987 and, therefore, a better template for the mutagenesis protocol used to insert the six-His tag. Attempts to make this insertion with the conventional protocol using Stratagene's QuikChange kit were unsuccessful. The protocol was modified by using the two-stage procedure of Wang and Malcom (*18*) to introduce the insertion that encodes the six-His tag by site-directed mutagenesis. Briefly, an extension reaction was performed with the pMEG985 template and each primer separately, for three cycles; then the contents of the two reaction solutions were mixed, and the standard reaction was carried out for another 25 cycles. The primers that were used were 5′-CCTATCACTGCACGATCTCCCCCATCGTGGGCA-AGGCGAGCCACCACCACCACCACCACTGACGGC-GGCCGGGCGCGCATGC-3′ and its complementary DNA. The inserted nucleotides are underlined. After introduction of the insertion by this mutagenesis procedure, the *Eco*RI fragment was excised and ligated back into pMEG987 in place of the original *Eco*RI fragment. The resulting plasmid, pMEG976, was used directly for further site-directed mutagenesis reactions. For expression in *R. sphaeroides*, pMEG976 was digested with *Kpn*I to isolate the entire

coxIIpromoter-*mauFBEDA(6xHis)CJG* region which controls protein expression and biosynthesis, and this region was inserted into the broad-host-range vector pRK415-1, creating pMEG975.

Upon sequencing of the 3′ end of *mauA* and the intergenic region between *mauA* and *mauC*, we found that two copies of the primers used to insert the six-His tag had in fact been inserted. However, since the second copy of the primer was after the stop codon for *mauA*, and before the ribosome binding site for *mauC*, this extra copy did not affect expression of the proteins.

Site-Directed Mutagenesis of MADH on pMEG976. Site-directed mutagenesis was performed on double-stranded pMEG976 using the primers described above with Stratagene's QuikChange kit with the following modifications. The reaction mixture contained 2% formamide and 5% dimethyl sulfoxide, which improved the PCR for large plasmids. The site-directed mutagenesis of Asp180 of the MADH α subunit to Arg was performed as follows. The pair of primers used to create the mutation were 5′-GCGC-ATGCTGGACGTGCCTAGGTGCTATCACATCTTCC-3′ and its complementary DNA. The four underlined bases which were changed also created a unique *Avr*II site which did not exist in pMEG976. This facilitated screening for the mutant by restriction digest. The mutation was then confirmed by sequencing 70 base pairs around the mutated site. The *Kpn*I fragment of this mutated plasmid was excised and cloned into PRK415-1, to yield pZZ102, which was used for expression of αD180R MADH in *R. sphaeroides*.

Purification of 6xHis-MADH. The methods for growth of *R. sphaeroides* and preparation of the periplasmic fraction of these cells after harvest were as described previously (*16*, *17*). The periplasm was concentrated by ultrafiltration and exchanged with the buffer [50 mM NaH_2PO_4 (pH 8.0), 300 mM NaCl, and 10 mM imidazole] used to equilibrated the chromatography column that was used in the subsequent purification. The sample was applied to a Ni^{2+}−NTA superflow column (Qiagen) (2 mL of resin/100 g of cells). The column was washed with 5 column volumes of the equilibration buffer and then eluted with buffer that contained increasing concentrations of imidazole. The 6xHis-MADH eluted at approximately 50 mM imidazole.

Kinetic Analysis of Native, Recombinant, Six-His-Tagged, and Mutant MADH. Steady-state kinetic experiments with PES as an electron acceptor for MADH were performed essentially as described previously (*16*). The assay mixture contained 16 nM MADH, various concentrations of methylamine, 4.8 mM PES, and 170 μM DCIP, in 0.1 M KP_i at pH 7.5 and 30 °C. The reactions were started by addition of methylamine, and activity was monitored by the decrease in absorbance at 600 nm due to reduction of DCIP. In this way, the reactivities of different forms of MADH toward the substrate methylamine were compared.

Steady-state kinetic experiments with amicyanin as a terminal electron acceptor were performed essentially as described previously (*6*). The assay mixture contained 16 nM MADH and various concentrations of native or mutant amicyanin in 10 mM KP_i at pH 7.5, with or without 200 mM KCl, at 30 °C. The reaction was initiated by the addition of 0.1 mM methylamine, and activity was monitored by the change in absorbance at 600 nm caused by the reduction of amicyanin. Data from steady-state kinetic experiments were

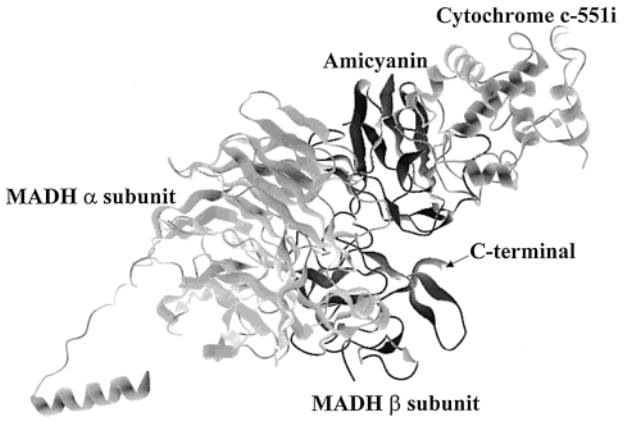

FIGURE 1: Crystal structure of the ternary protein complex of MADH, amicyanin, and cytochrome c_{551i}. Only half of the complex with one subunit each from MADH is shown. The C-terminus of β subunit of MADH, which is the site of addition of the six-His tag, is indicated. The coordinates are available as Protein Data Bank entry 2MTA.

fit to eq 2

$$v/E = k_{cat}[S]/(K_m + [S]) \quad (2)$$

where v is the measured initial reaction rate, E is the concentration of MADH, [S] is the concentration of methylamine or amicyanin, k_{cat} is the turnover number, and K_m is the Michaelis−Menten constant.

Molecular Modeling. The crystal structures that were analyzed were those of free MADH (*13*; PDB entry 2BBK), free amicyanin (*14*; PDB entry 1AAC), and the MADH−amicyanin−cytochrome c_{551i} complex (*15*; PDB entry 2MTA). Manipulation and comparisons of these structures were performed using the QUANTA and CHARMm (Molecular Simulations) computer programs run on a Silicon Graphics O2 computer.

RESULTS

Expression and Properties of 6xHis-MADH. The expression level of 6xHis-MADH, based on the yield of purified protein, was approximately one-third (10 mg/100 g wet weight of cells) of that of the untagged native recombinant MADH expressed in *R. sphaeroides*. Although the reason for this somewhat lower yield is unknown, it is clear that the addition of the six-His tag to the C-terminal end of the β subunit did not prevent the biosynthesis of this subunit, its export to the periplasm, or correct assembly of subunits to form the holoenzyme. This is consistent with the known structure of MADH which reveals that the C-terminus of the small subunit is at the surface of the protein and away from the subunit interface (Figure 1). The 6xHis-MADH was constructed not only to make the purification of the recombinant protein easier but also to facilitate the purification of mutant enzymes without activity or with altered spectral properties. Thus, the advantages afforded by the addition of the six-His tag outweigh the lower yields.

The visible spectrum of MADH arises from the TTQ cofactor in the β subunit, and each of the three redox forms of MADH exhibits distinct spectra (*19*). The spectra of the oxidized, semiquinone, and reduced forms of 6xHis-MADH were indistinguishable from those of native MADH. The steady-state kinetic parameters for the reactions of 6xHis-

Table 2: Comparison of Kinetic Parameters of 6xHis-MADH with Those of Native MADH

kinetic parameter	electron acceptor	6xHis-MADH	native MADH
k_{cat} (s^{-1})	PES/DCIP	18.4 ± 1.3	13.6 ± 0.1
K_m (μM) with methylamine	PES/DCIP	5.9 ± 0.5	6.4 ± 0.2
k_{cat} (s^{-1})	amicyanin	62.2 ± 3.1	61 ± 6.0
K_m (μM) with amicyanin	amicyanin	6.7 ± 1.1	3.6 ± 1.9

Table 3: Kinetic Parameters for Methylamine Oxidation by αD180R MADH and Native MADH with Artificial Electron Acceptors

MADH	k_{cat} (s^{-1})	K_m (μM) with methylamine
native	13.6 ± 0.1	6.4 ± 0.2
αD180R	13.6 ± 0.5	5.9 ± 0.3

Table 4: Effects of Mutations on the K_m Values for the Reaction of MADH with Amicyanin

		K_m (μM) for amicyanin	
MADH	amicyanin	10 mM KP_i at pH 7.5	10 mM KP_i and 0.2 M KCl
native	native	1.3 ± 0.3[a]	8.0 ± 1.2[a]
αD180R	native	527 ± 127	650 ± 176
native	R99D	76.1 ± 8.8[a]	63.9 ± 6.6[a]
αD180R	R99D	1230 ± 286	1290 ± 300
αD180R	R99L	1263 ± 225	1144 ± 153

[a] Taken from ref *7*.

MADH were compared with those of the native enzyme and shown to be very similar (Table 2). It is important in this study to verify that the six-His tag does not significantly affect the interaction between MADH and amicyanin. Again, this observation is consistent with the crystal structure of the MADH−amicyanin−cytochrome c_{551i} complex that indicates that the C-terminus of the β subunit of MADH is located on the protein surface in a region where one would not expect it to interact with residues at the MADH−amicyanin interface (Figure 1).

Expression and Properties of αD180R MADH. The expression level of αD180R 6xHis-MADH, based on the yield of purified protein, was approximately equal to that of the 6xHis-MADH expressed in *R. sphaeroides*. The visible spectra of the oxidized, semiquinone, and reduced forms of the αD180R MADH were indistinguishable from that of native MADH. This suggests that the mutation has not affected the electronic properties of the TTQ prosthetic group.

The steady-state kinetic parameters for the reactions of αD180R MADH were compared with those of the native enzyme (Table 3). When the artificial electron acceptor, PES, is used in the steady-state assay, the values of k_{cat} and K_m for methylamine were essentially the same as for native MADH. This indicates that the αD180R mutation, which is at the surface of MADH, has not affected the substrate binding and catalytic reactions that occur at the active site of MADH. However, significant differences were observed between αD180R and native MADH in the steady-state reaction with amicyanin as the electron acceptor (Table 4). The K_m value for amicyanin increased approximately 400-fold as a result of the αD180R mutation. Furthermore, the mutation eliminated the ionic strength dependence of the K_m value for amicyanin which is observed for the reaction of native MADH with amicyanin. Whereas with the native MADH this K_m value increased more than 6-fold on addition of 0.2 M KCl to the 10 mM KP_i buffer, no increase in this K_m value was observed with the αD180R mutant.

FIGURE 2: Location of the interprotein salt bridge at the MADH−amicyanin interface. This is an enlarged view of the relevant portion of the structure displayed in Figure 1. Amicyanin residues Arg99 and Phe97, and MADH residue αAsp180, are displayed as ball-and-stick models and are labeled.

Reactions of αD180R MADH with R99D and R99L Amicyanin. Since residues αAsp180 of MADH and Arg99 of amicyanin are seen in the crystal structure of the protein complex to form a salt bridge (Figure 2), we examined whether the R99D mutation of amicyanin could complement the αD180R mutation of MADH and restore wild-type binding affinity (Table 4). Interestingly, the K_m value for the reaction of αD180R MADH with R99D amicyanin is almost 1000-fold greater than of the reaction between the native proteins, and also much greater than the K_m values for reactions between mutant and native proteins. A similar very large K_m value was obtained for the steady-state reaction of αD180R MADH with another mutant, R99L amicyanin. Neither of these K_m values for the reactions of the mutant amicyanins with αD180R MADH exhibited any ionic strength dependence. Despite the large differences in K_m values, the k_{cat} values for turnover in these steady-state reactions were similar. The k_{cat} for the reaction of αD180R MADH with R99D amicyanin was 87 ± 21 s^{-1} compared to 66 ± 1 s^{-1} for the wild type under low-salt conditions, and 117 ± 5 s^{-1} compared to 119 ± 15 s^{-1} in the presence of 200 mM KCl.

DISCUSSION

Molecular Basis of the Mutation Effect on Binding of MADH and Amicyanin. Interprotein salt bridges have been implicated in helping to stabilize certain protein−protein interactions that are important in protein binding and function. Amino acid residues that appear to participate in interprotein salt bridges are attractive targets for site-directed mutagenesis. When mutation of such a residue disrupts function, it is usually taken as evidence for the importance of the ionic interaction. This is as far as such studies usually go. Intuitively, one would expect that if each of the residues that participates in an interprotein salt bridge were mutated to the other residue, such an inverse pair of mutations would complement each other and restore activity. The ionic interaction of the oppositely charged residues is nondirectional, so it should not matter which residue is on which

protein for the salt bridge to form. An example of this was reported for the lactose permease (*20*) where single mutations of D237 or K358 abolished activity, but a D237K/K358D double mutation was active. In that case, the neutralized charge pair appeared to be important for proper insertion of the protein into the membrane. However, such complementation by inverse mutation is not necessarily the case. A computational analysis of conservation of salt bridges in protein families revealed that the compensation mode of conservation (i.e., reversal of charges) occurs only rarely (*21*). An experimental example of the inability to restore an interprotein salt bridge by such compensation involves the interaction between lipase and colipase (*22*), which is stabilized by an interprotein ion pair that is critical for catalysis. Mutation of either residue involved in the ion pair significantly disrupted activity. However, the inverse mutations of lipase K400E and colipase E45K did not have a compensatory effect. In fact, the interaction of the two mutants was somewhat worse than that of either mutant with the wild type (*22*). An even more extreme example of the inability of inverse mutations to restore an interprotein salt bridge is described in our study with MADH and amicyanin. In this discussion, molecular modeling and thermodynamic analysis of the kinetic data are used to elucidate the molecular basis for these observations.

The K_m values obtained from the steady-state analysis of the reactions of amicyanin with MADH mutants are listed in Table 4. In previous studies, we have been able to obtain K_d values for the wild-type MADH−amicyanin complex, and the complexes with some amicyanin mutants, from the analysis of transient kinetic data (*7*, *23*, *24*). Unfortunately, the interaction of the αD180R MADH with amicyanin is so weak that it was not possible to use sufficiently high protein concentrations in the transient kinetic studies to approach saturation kinetics so that an accurate K_d value could be obtained (data not shown). Such studies are done by stopped-flow spectroscopy. At the high protein concentrations that are required, particularly for the reactions of αD180R MADH with mutant amicyanins (i.e., K_m > 1 mM), the high background absorbance and viscosity of the very concentrated protein solution, as well as the prohibitive amount of protein required for complete studies, made the precise determination of K_d values not feasible. Fortunately, our previous studies with amicyanin mutants demonstrated that the correlation between steady-state K_m values and true K_d values is quite good. In particular, the correlation between ΔK_m and ΔK_d values for complex formation between MADH and different amicyanin mutants is quite strong (*7*). Thus, the differences in K_m values reported in Table 4 are a reasonable estimation of the relative affinities of these wild-type and mutant proteins.

The order of affinity for native and mutant proteins that was observed in this study was as follows: native MADH and native amicyanin > native MADH and R99D amicyanin > αD180R MADH and native amicyanin > αD180R MADH and R99D amicyanin, and αD180R MADH and R99L amicyanin. In MADH, residue α179 is a proline and residue α181 is a cysteine that participates in a disulfide bond. Thus, the α180 residue (Arg in the wild type and Asp in the mutant) is spatially restricted in its movement. This provides one clue as to why simply performing the inverse pair of mutations does not restore activity. It does not explain,

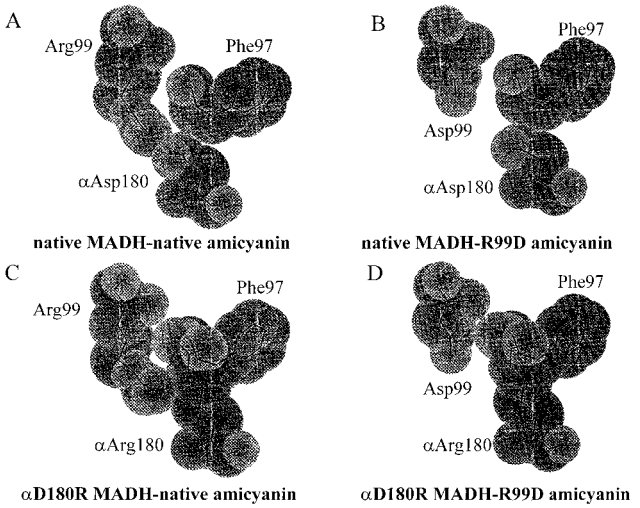

FIGURE 3: Interactions between residues 99 of amicyanin and α180 of MADH in native and mutant protein complexes. The positions of Arg99, αAsp180, and Phe97 of amicyanin in the native complex are shown in panel A, with van der Waals radii indicated by the gray spheres. The coordinates are available as Protein Data Bank entry 2MTA. In panels B−D, the positions of mutated residues have been modeled into the wild-type structure as described in Experimental Procedures. The details of the interactions that are revealed by these structures are described in detail in the text.

however, why the interactions of αD180R MADH with amicyanin are so much weaker than interactions of mutant amicyanins with MADH. With such weak interactions, it was not possible to obtain structures of the complexes. Modeling of these mutations into the MADH−amicyanin complex structure (Figure 3) does provide some insight into this phenomenon.

There is a salt bridge between Arg99 of amicyanin and αAsp180 of MADH in the native protein complex (Figure 3A), which is to say, the side chain NH2 of Arg99 is separated by 2.7 Å from the OD1 and OD2 of αAsp180. This salt bridge is lost in the native MADH−R99D amicyanin complex (Figure 3B). This salt bridge is also lost in the αD167R MADH−native amicyanin complex, but that mutation also generates two additional significant interactions (Figure 3C). αArg180 forms an unfavorable interaction with Phe97 on amicyanin. The side chain NH2 of αArg180 is predicted to come within 0.7 Å of the O of Phe97 and, therefore, have a significant destabilizing influence on complex formation. If the side chain of αArg180 is rotated about its $C_\alpha-C_\beta$ bond, it is not possible to assume a conformation that is devoid of unfavorable close contacts. Conversely, in the conformation shown in Figure 3C, αArg180 also forms a favorable van der Waals interaction with Arg99 on amicyanin. This involves the carbons of the two arginine side chains. In the αD180R MADH−R99D amicyanin complex (Figure 3D), the unfavorable interaction between αArg180 and Phe97 remains, but the favorable van der Waals interaction that was seen in Figure 3C is lost. This accounts for the even weaker affinity of the inverse mutant pair. A new salt bridge between αArg180 on αD180R MADH and Asp99 on R99D amicyanin does not form because the distance between the residues is too large. This is in large part due to the restricted mobility of the side chain of the residue at the 180α position, which was discussed earlier. The same thing is observed for the interaction of αD180R MADH with R99L amicyanin (not shown) where

Table 5: Energy Differences for Complex Formation[a]

complexes being compared	$\Delta\Delta G°$ relative to the wild type (kcal/mol)
native MADH−R99D amicyanin	2.4
αD180R MADH−native amicyanin	3.6
αD180R MADH−R99D amicyanin	4.1
αD180R MADH−R99L amicyanin	4.1

[a] $\Delta\Delta G°$ values are for complex formation in 10 mM KP_i at pH 7.5 in the absence of added KCl.

leucine is unable to move close enough to αArg180 to participate in any stabilizing interactions.

Thermodynamic Consequences of Mutations. Thermodynamic calculations were performed to gain further insight into how the interactions observed in the molecular modeling studies correlate with the observed differences in affinity for these proteins. The energy difference of two binding reactions can be calculated according to eq 3

$$\Delta\Delta G° = -RT \ln(K_{eq1}/K_{eq2}) = -RT \ln(K_{d2}/K_{d1}) \quad (3)$$

where $\Delta\Delta G°$ is the binding free energy difference, R is the gas constant, and T is the temperature. K_{eq1} and K_{eq2} are the equilibrium constants for complex formation between the proteins and are the reciprocals of the dissociation constants K_{d1} and K_{d2}, respectively. As discussed earlier, it was not possible to directly measure K_d values in this study, but previous studies indicated that ΔK_m values for these complexes correlate well with ΔK_d values (*7*). Therefore, in these calculations, the K_m values listed in Table 4 were used in place of K_d values in eq 3. The $\Delta\Delta G°$ values which correspond to the destabilization of the complex by site-directed mutations are listed in Table 5.

If the major consequence of the R99D mutation of amicyanin is to eliminate the salt bridge that stabilizes the wild-type complex (Figure 3B), then the analysis by eq 3 indicates that this salt bridge contributes about 2.4 kcal/mol toward stabilization of the complex. It should be noted that the K_m value for the reaction of native MADH with R99D amicyanin in low salt is significantly higher than that of the wild-type complex in 0.2 M KCl. That is because in 0.2 M KCl the native salt bridge is only partially disrupted. The unfavorable close contact between αArg180 and Phe97 of amicyanin in the complexes with αD180R MADH (Figure 3C,D) contributes an additional 1.7 kcal/mol toward destabilization of the complex. The apparent favorable van der Waals interaction between αArg180 and Arg99 in the αD180R MADH−native amicyanin complex provides a stabilization of 0.5 kcal/mol.

Sequential Model for the Interaction of MADH with Amicyanin. While the identity of the residues which participate in the MADH−amicyanin interface and the forces which stabilize the protein−protein interaction are well characterized, the sequences of events which lead to formation of the MADH−amicyanin complex remains unclear. In addition to the salt bridge that has been studied here, other hydrophobic interactions are also critical (*7*). It has been proposed that the recognition and formation of the salt bridge precedes and helps to orient the residues for the hydrophobic interaction (*7*). However, the new information presented here suggests an alternative model.

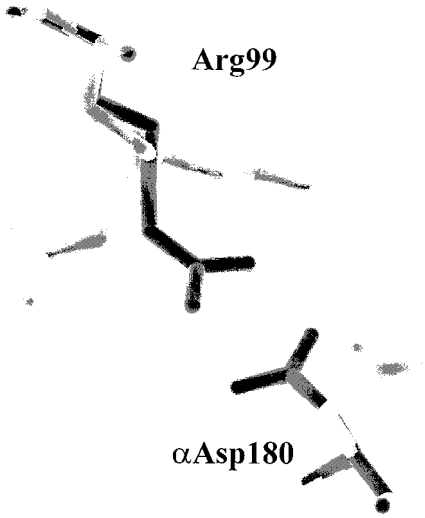

FIGURE 4: Comparison of the positions of Arg99 of amicyanin and αAsp180 of MADH when the proteins are free and in complex. The structures used in this comparison are free MADH (PDB entry 2BBK), free amicyanin (PDB entry 1AAC), and the MADH−amicyanin complex (PDB entry 2MTA). The positions of these residues in the protein complex are indicated in black, and the positions of the residues in the uncomplexed proteins are indicated in gray. As discussed in the text, in free amicyanin Arg99 assumes two alternative conformations, both of which are shown.

Comparison of the structures of MADH and amicyanin free and in complex indicates that the amino acid residues which are present at the hydrophobic interface move very little on complex formation whereas the positions of the residues which participate in the salt bridge at the periphery of the hydrophobic interface shift significantly. The positions of Arg99 of amicyanin and αAsp180 of MADH are shown in Figure 4. In the free amicyanin structure, Arg99 assumes two different conformations, neither of which is the same as when it is in complex. The side chain of αAsp180 also exhibits a significant rotation about its $C_\alpha-C_\beta$ bond that repositions the carboxylic oxygen by about 3 Å. If the ionic interaction between these residues preceded the hydrophobic interactions, one would not expect this significant shift in position. An initial hydrophobic interaction, followed by repositioning of Arg99 and αAsp180 to form the salt bridge, seems more likely. This scenario is further supported by the results obtained for the reactions of R99D amicyanin with αD180R MADH. If salt bridge formation preceded the hydrophobic interaction, one would expect that the inverse mutation pair could recover the salt bridge, since the free proteins could orient themselves to bring these residues together. On the contrary, if the formation of the hydrophobic interactions precedes salt bridge formation, then the salt bridge cannot form in the mutant complex because the movement of the side chain of αArg180 is confined (discussed earlier). The notion that the hydrophobic, rather than the ionic interactions, is the initial determinant in complex formation is also supported by the results of a van't Hoff analysis of the binding of wild-type amicyanin and MADH (*22*). These results indicated that the $\Delta H°$ for binding was relatively small and that the association was primarily driven by $\Delta S°$. This is consistent with the desolvation of hydrophobic residues on protein association providing much of the driving force for complex formation. The fact that the protein complex was crystallized in very high salt (*4*,

25) is also consistent with this scenario for protein association. An alternative interpretation is that the native salt bridge does normally guide and precede hydrophobic interactions, but the artificial inverse salt bridge forms and guides a wrong complex that is weak or incapable of efficient electron transfer. This latter alternative seems unlikely since similar k_{cat} values were obtained for the steady-state reactions of the native and R99D amicyanin−αD180R MADH complexes. Thus, the most likely model for complex formation is one in which hydrophobic association precedes formation of the salt bridge between Arg99 on amicyanin and αAsp180 on MADH. The initial hydrophobic interaction mainly determines the on rate for complex formation, and the salt bridge, once formed, stabilizes the complex by decreasing the off rate for dissociation of the complex.

Conclusion. Methods were developed for the construction and heterologous expression of a six-His-tagged MADH and site-directed mutagenesis of this protein. Mutation of αAsp180 on MADH destabilized the complex to a much greater degree than mutation of Arg99 on amicyanin. Inverse mutation of the pair did not restore wild-type binding, but weakened the affinity of the proteins more severely than either individual mutation. Molecular modeling studies and energy calculations provided a molecular basis for these observations and illustrated how subtle perturbations of specific features of the protein structure can have large effects on the strength of specific protein−protein interactions.

ACKNOWLEDGMENT

We thank Bethel Sharma and Stephanie Warren for technical assistance in cell culture and protein purification.

REFERENCES

1. Davidson, V. L. (1993) in *Principles and Applications of Quinoproteins* (Davidson, V. L., Ed.) pp 73−95, Marcel Dekker, New York.
2. McIntire, W. S., Wemmer, D. E., Christoserdov, A. Y., and Lindstrom, M. E. (1991) *Science 252*, 817−824.
3. Husain, M., and Davidson, V. L. (1985) *J. Biol. Chem. 260*, 14626−14629.
4. Chen, L., Durley, R. C. E., Poloks, B. J., Hamada, K., Chen, Z., Mathews, F. S., Davidson, V. L., Satow, Y., Huizinga, E., Vellieux, F. M. D., and Hol, W. G. J. (1992) *Biochemistry 31*, 4959−4964.
5. Davidson, V. L., Graichen, M. E., and Jones, L. H. (1993) *Biochim. Biophys. Acta 1144*, 39−45.
6. Brooks, H. B., Jones, L. H., and Davidson, V. L. (1993) *Biochemistry 32*, 2725−2729.
7. Davidson, V. L., Jones, L. H., Graichen, M. E., Mathews, F. S., and Hosler, J. P. (1997) *Biochemistry 36*, 12733−12738.
8. Brooks, H. B., and Davidson, V. L. (1994) *J. Am. Chem. Soc. 116*, 11201−11202.
9. Bishop, G. R., and Davidson, V. L. (1997) *Biochemistry 36*, 13586−13592.
10. Bishop, G. R., and Davidson, V. L. (1998) *Biochemistry 37*, 11026−11032.
11. Zhu, Z., and Davidson, V. L. (1999) *Biochemistry 38*, 4862−4867.
12. Zhu, Z., Cunane, L. M., Chen, Z.-W., Durley, R. C. E., Mathews, F. S., and Davidson, V. L. (1998) *Biochemistry 37*, 17128−17136.
13. Chen, L., Doi, M., Durley, R. C. E., Chistoserdov, A. Y., Lidstrom, M. E., Davidson, V. L., and Mathews, F. S. (1998) *J. Mol. Biol. 276*, 131−149.
14. Cunane, L. M., Chen, Z.-W., Durley, R. C. E., and Mathews, F. S. (1996) *Acta Crystallogr. D52*, 676−686.
15. Chen, L., Durley, R. C. E., Mathews, F. S., and Davidson, V. L. (1994) *Science 264*, 86−90.
16. Graichen, M. E., Jones, L. H., Sharma, B. V., van Spanning, R. J. M., Hosler, J. P., and Davidson, V. L. (1999) *J. Bacteriol. 181*, 4216−4222.
17. Davidson, V. L. (1990) *Methods Enzymol. 188*, 241−246.
18. Wang, W., and Malcolm, B. A. (1999) *BioTechniques 26*, 680−682.
19. Davidson, V. L., Brooks, H. B., Graichen, M. E., Jones, L. H., and Hyun, Y. (1995) *Methods Enzymol. 258*, 176−190.
20. Dunten, R. L., Sahin-Toth, M., and Kaback, H. R. (1993) *Biochemistry 32*, 3139−3145.
21. Schueler, O., and Margalit, H. (1995) *J. Mol. Biol. 248*, 125−135.
22. Ayvazian, L., Crenon, I., Hermoso, J., Pignol, D., Chapus, C., and Kerfelec, B. (1998) *J. Biol. Chem. 273*, 33604−33609.
23. Brooks, H. B., and Davidson, V. L. (1994) *Biochemistry 33*, 5696−5701.
24. Davidson, V. L., Jones, L. H., and Zhu, Z. (1998) *Biochemistry 37*, 7371−7377.
25. Chen, L., Mathews, F. S., Davidson, V. L., Tegoni, M., Rivett, C., and Rossi, L. (1993) *Protein Sci. 2*, 147−154.
26. Simon, R., Priefer, U., and Puhler, A. (1983) *Bio/Technology 1*, 784−791.
27. Keen, N. T., Tamaki, S., Kobayashi, D., and Trollinger, D. (1988) *Gene 70*, 191−197.

BI000502P